

Temperature dependence of gain and excess noise in InAs electron avalanche photodiodes

Pin Jern Ker, John P. R. David, and Chee Hing Tan*

Department of Electronic and Electrical Engineering, The University of Sheffield, Sir Frederick Mappin Building, Mappin Street, Sheffield. S1 3JD, UK

*c.h.tan@sheffield.ac.uk

Abstract: Measurement and analysis of the temperature dependence of avalanche gain and excess noise in InAs electron avalanche photodiodes (eAPDs) at 77 to 250 K are reported. The avalanche gain, initiated by pure electron injection, was found to reduce with decreasing temperature. However no significant change in the excess noise was measured as the temperature was varied. For avalanche gain > 3 , the InAs APDs with 3.5 μm i -region show consistently low excess noise factors between 1.45 and 1.6 at temperatures of 77 to 250 K, confirming that the eAPD characteristics are exhibited in the measured range of electric field. As the dark current drops much more rapidly than the avalanche gain and the excess noise remains very low, our results confirmed that improved signal to noise ratio can be obtained in InAs eAPDs by reducing the operating temperature. The lack of hole impact ionization, as confirmed by the very low excess noise and the exponentially rising avalanche gain, suggests that hole impact ionization enhancement due to band “resonance” does not occur in InAs APDs at the reported temperatures.

©2012 Optical Society of America

OCIS codes: (040.1345) Avalanche photodiodes (APDs); (250.0040) Detectors.

References and links

1. J. P. R. David and C. H. Tan, “Material considerations for avalanche photodiodes,” *IEEE J. Sel. Top. Quantum Electron.* **14**(4), 998–1009 (2008).
2. G. J. Rees and J. P. R. David, “Why small avalanche photodiodes are beautiful,” *Proc. SPIE* **4999**, 349–362 (2003).
3. R. J. McIntyre, “Multiplication noise in uniform avalanche diodes,” *IEEE Trans. Electron. Dev.* **13**(1), 164–168 (1966).
4. A. R. J. Marshall, C. H. Tan, M. J. Steer, and J. P. R. David, “Electron dominated impact ionization and avalanche gain characteristics in InAs photodiodes,” *Appl. Phys. Lett.* **93**, 111107 (2008).
5. A. R. J. Marshall, C. H. Tan, M. J. Steer, and J. P. R. David, “Extremely low excess noise in InAs electron avalanche photodiodes,” *IEEE Photon. Technol. Lett.* **21**(13), 866–868 (2009).
6. J. Beck, C. Wan, M. Kinch, J. Robinson, P. Mitra, R. Scritchfield, F. Ma, and J. Campbell, “The HgCdTe electron avalanche photodiode,” *J. Electron. Mater.* **35**(6), 1166–1173 (2006).
7. A. R. J. Marshall, P. J. Ker, A. Krysa, J. P. R. David, and C. H. Tan, “High speed InAs electron avalanche photodiodes overcome the conventional gain-bandwidth product limit,” *Opt. Express* **19**(23), 23341–23349 (2011).
8. S. J. Maddox, W. Sun, Z. Lu, H. P. Nair, J. C. Campbell, and S. R. Bank, “Enhanced low-noise gain from InAs avalanche photodiodes with reduced dark current and background doping,” *Appl. Phys. Lett.* **101**, 151124 (2012).
9. P. J. Ker, A. R. J. Marshall, A. B. Krysa, J. P. R. David, and C. H. Tan, “Temperature dependence of leakage current in InAs avalanche photodiodes,” *IEEE J. Quantum Electron.* **47**(8), 1123–1128 (2011).
10. A. R. J. Marshall, P. Vines, P. J. Ker, J. P. R. David, and C. H. Tan, “Avalanche multiplication and excess noise in InAs electron avalanche photodiodes at 77 K,” *IEEE J. Quantum Electron.* **47**(6), 858–864 (2011).
11. D. J. Massey, J. P. R. David, and G. J. Rees, “Temperature dependence of impact ionization in submicrometer silicon devices,” *IEEE Trans. Electron. Dev.* **53**(9), 2328–2334 (2006).
12. C. Groves, R. Ghin, J. P. R. David, and G. J. Rees, “Temperature dependence of impact ionization in GaAs,” *IEEE Trans. Electron. Dev.* **50**(10), 2027–2031 (2003).
13. L. J. J. Tan, D. S. G. Ong, J. S. Ng, C. H. Tan, S. K. Jones, Q. Yahong, and J. P. R. David, “Temperature dependence of avalanche breakdown in InP and InAlAs,” *IEEE J. Quantum Electron.* **46**(8), 1153–1157 (2010).

14. C. L. F. Ma, M. J. Deen, L. E. Tarof, and J. C. H. Yu, "Temperature dependence of breakdown voltages in separate absorption, grading, charge, and multiplication InP/InGaAs avalanche photodiodes," *IEEE Trans. Electron. Dev.* **42**(5), 810–818 (1995).
15. H. Kanbe, "Temperature dependence of multiplication noise in Silicon avalanche photodiodes," *Electron. Lett.* **14**(17), 539–541 (1978).
16. J. Yu, L. E. Tarof, R. Bruce, D. G. Knight, K. Visvanatha, and T. Baird, "Noise performance of separate absorption, grading, charge and multiplication InP/InGaAs avalanche photodiodes," *IEEE Photon. Technol. Lett.* **6**(5), 632–634 (1994).
17. Y. G. Xiao and M. J. Deen, "Temperature dependent studies of InP/InGaAs avalanche photodiodes based on time domain modeling," *IEEE Trans. Electron. Dev.* **48**(4), 661–670 (2001).
18. X. G. Zheng, P. Yuan, X. Sun, G. S. Kinsey, A. L. Holmes, B. G. Streetman, and J. C. Campbell, "Temperature dependence of the ionization coefficients of $\text{Al}_x\text{Ga}_{1-x}\text{As}$," *IEEE J. Quantum Electron.* **36**(10), 1168–1173 (2000).
19. M. P. Mikhailova, M. M. Smirnova, and S. V. Slobodchikov, "Carrier multiplication in InAs and InGaAs p-n junctions and their ionization coefficients," *Sov. Phys. Semicond.* **10**, 509–513 (1976).
20. P. Norton, "HgCdTe infrared detectors," *Opto-Electron. Rev.* **10**, 159–174 (2002).
21. C. H. Grein and H. Ehrenreich, "Impact ionization enhancements in $\text{Al}_x\text{Ga}_{1-x}\text{Sb}$ avalanche photodiodes," *Appl. Phys. Lett.* **77**(19), 3048–3050 (2000).
22. Z. M. Fang, K. Y. Ma, D. H. Jaw, R. M. Cohen, and G. B. Stringfellow, "Photoluminescence of InSb, InAs, and InAsSb grown by organometallic vapor phase epitaxy," *J. Appl. Phys.* **67**(11), 7034–7039 (1990).
23. I. Vurgaftman, J. R. Meyer, and L. R. Ram-Mohan, "Band parameters for III–V compound semiconductors and their alloys," *J. Appl. Phys.* **89**(11), 5815–5875 (2001).
24. A. R. J. Marshall, C. H. Tan, J. P. R. David, J. S. Ng, and M. Hopkinson, "Fabrication of InAs photodiodes with reduced surface leakage current," *Proc. SPIE* **6740**, 67400H (2007).
25. S. Adachi, "Optical dispersion relations for GaP, GaAs, GaSb, InP, InAs, InSb, $\text{Al}_x\text{Ga}_{1-x}\text{As}$, and $\text{In}_{1-x}\text{Ga}_x\text{As}_y\text{P}_{1-y}$," *J. Appl. Phys.* **66**(12), 6030–6040 (1989).
26. J. Bude and K. Hess, "Thresholds of impact ionization in semiconductors," *J. Appl. Phys.* **72**(8), 3554–3561 (1992).
27. C. H. Tan, G. J. Rees, P. A. Houston, J. S. Ng, W. K. Ng, and J. P. R. David, "Temperature dependence of electron impact ionization in $\text{In}_{0.53}\text{Ga}_{0.47}\text{As}$," *Appl. Phys. Lett.* **84**(13), 2322–2324 (2004).
28. J. R. Chelikowsky and M. L. Cohen, "Nonlocal pseudopotential calculations for the electronic structure of eleven diamond and zinc-blende semiconductors," *Phys. Rev. B* **14**(2), 556–582 (1976).
29. P. J. Ker, A. R. J. Marshall, J. P. R. David, and C. H. Tan, "Low noise high responsivity InAs electron avalanche photodiodes for infrared sensing," *Phys. Status Solidi* **9**(2 c), 310–313 (2012).
30. K. S. Lau, C. H. Tan, B. K. Ng, K. F. Li, R. C. Tozer, J. P. R. David, and G. J. Rees, "Excess noise measurement in avalanche photodiodes using a transimpedance amplifier front-end," *Meas. Sci. Technol.* **17**(7), 1941–1946 (2006).
31. V. G. Luppov, *Frequency response of low frequency probes* (Wilmington, MA: Janis Research Company 2012).
32. S. A. Plimmer, J. P. R. David, and D. S. Ong, "The merits and limitations of local impact ionization theory," *IEEE Trans. Electron. Dev.* **47**(5), 1080–1088 (2000).
33. B. E. A. Saleh, M. M. Hayat, and M. C. Teich, "Effect of dead space on the excess noise factor and time response of avalanche photodiodes," *IEEE Trans. Electron. Dev.* **37**(9), 1976–1984 (1990).
34. A. R. J. Marshall, J. P. R. David, and C. H. Tan, "Impact ionization in InAs electron avalanche photodiodes," *IEEE Trans. Electron. Dev.* **57**(10), 2631–2638 (2010).
35. D. S. Ong, K. F. Li, G. J. Rees, J. P. R. David, and P. N. Robson, "A simple model to determine multiplication and noise in avalanche photodiodes," *J. Appl. Phys.* **83**(6), 3426–3428 (1998).

1. Introduction

APDs can improve the signal to noise ratio of a detection system, provided that the shot noise contributed by the leakage current and the excess noise associated with the avalanche gain are relatively low compared to the noise of the external amplifier. The excess noise is largely dependent on the material properties of the avalanche region as described in detail by David *et al.* [1]. In most semiconductor materials with similar ionization coefficients, the avalanche width, W is designed to be as thin as possible to increase the bandwidth and to reduce the excess noise factors, F at a given mean avalanche gain, M [2]. Here, the effect of dead space, d , which is defined as the minimum distance a carrier needs to travel before gaining sufficient energy to impact ionize, is exploited to produce lower F .

While beneficial for excess noise reduction, reducing W increases the tunneling current considerably leading to a higher shot noise, particularly in narrow bandgap semiconductors. Depending on the bandgap energy, E_g of the material, this imposes a minimum acceptable W so that the tunneling current can be sufficiently suppressed. For detection at wavelengths $> 1.8 \mu\text{m}$, materials with $E_g < 0.68 \text{ eV}$ are needed. Thus, suppressing the tunneling current is not possible if W is reduced substantially to reduce F . This approach is impractical and it is

necessary to identify semiconductor materials with disparate ionization coefficients such that their hole to electron ionization coefficients ratio, k is as small as possible [3].

InAs eAPDs show the highly desirable electron-dominated photomultiplication leading to $k = 0$ and extremely low F [4, 5] at room temperature. Its electron-only ionization and minimal F characteristics are similar to those observed in HgCdTe eAPDs [6]. At low electric fields, $E < 100$ kV/cm, the electron ionization coefficients, α in both InAs and HgCdTe, are significantly higher than wide E_g semiconductors while their hole ionization coefficients, β are negligible, leading to extremely low F . The eAPD characteristics of InAs were also corroborated with extremely high gain-bandwidth product of 580 GHz [7].

To achieve low excess noise, the carrier type which ionizes more readily has to be injected into the high-field region to initiate the impact ionization process. For InAs, the photons were fully absorbed in the p -doped region, leading to pure electron injection into the depletion region. The room temperature excess avalanche noise factor under pure electron injection, F_e of InAs eAPDs was reported to be ~ 1.6 [5]. The low excess noise results were also reported by Maddox *et al.* recently [8]. Although they can provide M with very low F , the high leakage current of InAs eAPDs at room temperature, due to its small E_g , produces high shot noise. Fortunately the dark current was found to reduce substantially when the InAs diodes were cooled from room temperature to 77 K [9]. In addition to the reduced dark current, Marshall *et al.* [10] reported reduced pure electron initiated avalanche gain, M_e at 77 K, in contrast to most of the well-established APDs' technologies such as Si [11], GaAs [12], InP [13, 14] and InAlAs [13]. In this work, we will obtain an accurate temperature dependence of M_e for a wide temperature range from 77 to 295 K, such that the reduction in M_e and dark current with decreasing temperatures can be compared.

Moreover there are only limited studies on the temperature dependence of F . Kanbe reported that the measured F in Si APD increases slightly with temperatures, T [15]. For III-V semiconductors, both measured [16] and modeled [17] F of InGaAs/InP APDs were found to exhibit a similar trend. Al_xGa_{1-x}As APD with $x = 0$ to 0.4, on the other hand, were reported to have little variation of F within the accuracy of measurement as T changes [18]. For InAs eAPDs the only low temperature excess noise result was reported at 77 K by Marshall *et al.* [10]. F_e at 77 K was measured to be lower than that of room temperature and it was attributed to the increased ionization threshold energy, ξ_{th} and d at 77 K. However they did not rule out the possibility of measurement error in F_e . This is because for F_e to drop from ~ 1.6 (at 295 K [5]) to ~ 1.3 (at 77 K [10]), the increase in ξ_{th} has to be significantly larger than the increase in E_g (this will be discussed section 3.2). Therefore, in this work we report the first comprehensive measurement of excess noise over a wide range of temperatures to investigate the variation of F_e with T using an improved set-up and devices to minimize measurement error.

Besides the observed reduction in M_e , there appears to be contradicting results on the impact ionization behavior at 77 K. Mikhailova *et al.* reported the enhanced hole impact ionization as band "resonance" occurred [19] when the spin-orbit splitting of the valence band energy, Δ_{so} is almost equal to the E_g of InAs at 77 K. Similar phenomena was also discussed by Norton [20] for the short wave infrared HgCdTe APDs with $E_g \sim 0.9$ eV. Grein *et al.* [21] predicted that this effect could produce an enhancement of β in AlGaSb, but only at a low $E \sim 33$ kV/cm in his simulation. In contrast the reported M_e and F_e characteristics at 77 K by Marshall *et al.* suggest that holes do not impact ionize until $E > 70$ kV/cm [10]. However as T increases from 77 K to room temperature, E_g varies from 0.4 to 0.35 eV in InAs [22]. It is not obvious if the band "resonance" may occur as E_g shifts closer to the reported value of Δ_{so} at $T = 77$ to 200 K [23] and whether this will change the $F_e < 2$ observed in InAs eAPD. Hence we will analyze both the temperature dependence of M_e and F_e to verify whether the band "resonance" effect occurs in InAs.

2. Experimental details and results

An InAs *p-i-n* diode structure was used in this experiment. It was grown by molecular beam epitaxy (MBE) on a *p*-type InAs substrate. Figure 1 shows the schematic cross sectional view of the InAs *p-i-n* diode together with the doping concentration and thickness of each layer. The *p*-layer of this *p-i-n* diode consists of highly doped (Be: $> 2 \times 10^{18} \text{ cm}^{-3}$) layers of a 0.1 μm InAs contact layer, a 0.2 μm AlAs_{0.16}Sb_{0.84} electron diffusion blocking layer and a 0.7 μm of InAs absorption layer to provide pure electron injection at visible wavelengths. It has an undoped region of $\sim 3.5 \mu\text{m}$ followed by an *n*-region (Si: $\sim 2 \times 10^{18} \text{ cm}^{-3}$) of $\sim 2 \mu\text{m}$.

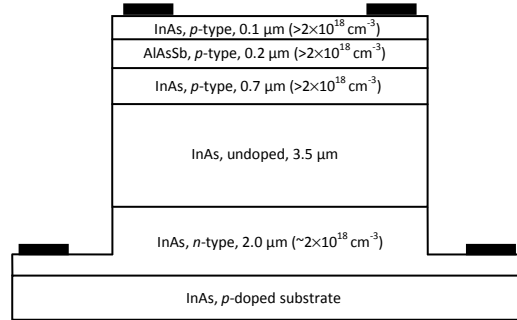


Fig. 1. Schematic cross sectional view of the InAs *p-i-n* diode.

The fabrication of mesa diode was carried out using the wet chemical etching reported in [24]. This InAs wafer was fabricated into circular mesa diodes with nominal diameters of 150 and 250 μm and passivated by SU-8 [9]. To enable the measurement of noise, ground-signal-ground (GSG) pads were deposited on the SU-8.

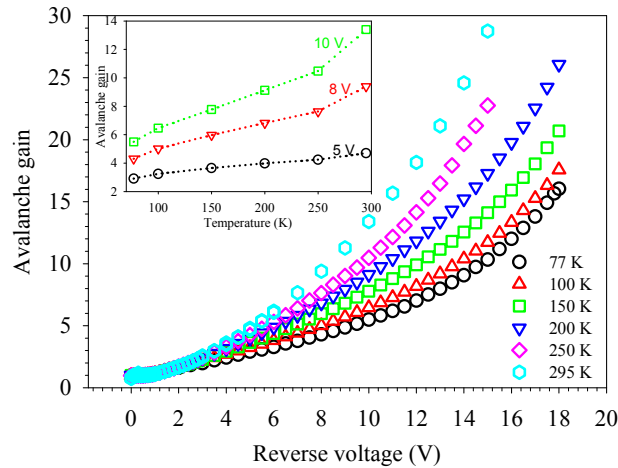


Fig. 2. Avalanche gain of the InAs *p-i-n* diode at 77, 100, 150, 200, 250 and 295 K. Inset shows the temperature dependent avalanche gain at different bias voltages.

The photomultiplication measurement was carried out using the phase sensitive detection (PSD) technique with a lock-in amplifier as it could differentiate the photocurrent from the dark current. The PSD allows us to extract the photocurrent accurately even in the presence of high dark current. To provide pure electron injection into the depletion region, the photons should be fully absorbed in the *p*-layer. As mentioned earlier, the InAs diodes have $\sim 1 \mu\text{m}$ thick *p*-layer. Based on the reported absorption coefficients [25], it is expected that $> 99\%$ of the 633-nm photons are absorbed in the InAs *p*-layer. M_e measured using 542-nm laser also showed good agreement with that using 633-nm laser confirming that pure electron injection was achieved. Measurements were also repeated with different levels of laser power to

eliminate the possibility of gain fluctuation due to heating. The measurement was repeated at $T = 77, 100, 150, 200, 250$ and 295 K. At each T , the $p-i-n$ diode exhibits exponentially rising M_e as shown in Fig. 2. It is clear that at a given bias voltage, V_b , M_e increases with T .

The experimental set-up for the noise measurement was similar to that used in [10] but two important changes were made. The noise figure meter was replaced by an Agilent 8973A noise figure analyzer (NFA) to allow measurement of the noise power over a wider frequency range and the devices were probed using a 50-GHz GSG probe which was connected to a bias-tee through a well-shielded cable with SMA connectors at both ends. The former enables verification that the noise measurement is independent of noise attenuation due to impedance mismatch while the latter is important to minimize interfering noise picked up by the two d.c. probes used in [10]. The d.c. bias voltage was applied to the APD via the bias-tee which also coupled the high frequency noise power generated by the APD into the NFA with an input impedance, $Z = 50 \Omega$. F was then determined by Eq. (1):

$$N_p = 2qI_{pr}M^2ZF \quad (1)$$

where N_p is the noise power measured by the NFA, q is the electron charge, and I_{pr} is the primary photocurrent. Pure electron injection was achieved by fiber-coupling the light onto the 250- μm diameter diode. Since this measurement set-up could not discriminate the photocurrent from the reverse leakage current, we ensured that the photocurrent was at least 2 orders of magnitude higher than the dark current. Examples of the photocurrent and dark current are shown in Fig. 3, together with its derived M_e at an intermediate $T = 200$ K. As shown in Eq. (1), the total noise power measured is the product of the multiplied shot noise and excess noise. However this is only applicable when I_{pr} is dominated by photocurrent, typically at least 100 times higher than the dark current in our measurements, to minimize error in F_e . Hence, F_e was measured at 77 to 250 K as the ratio of photocurrent to dark current at 295 K was not sufficiently large to obtain accurate value of F_e .

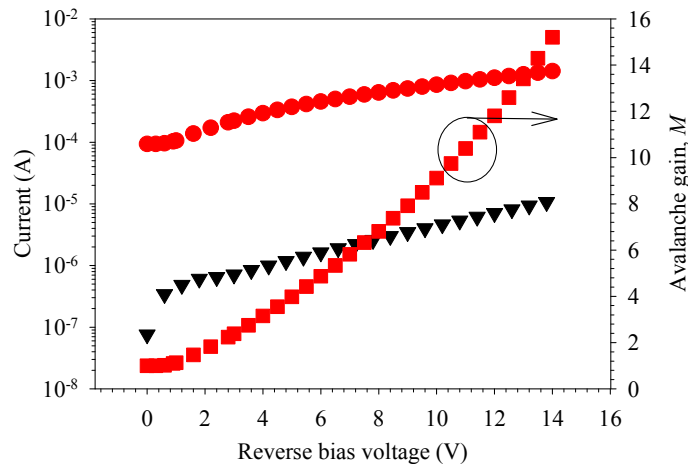


Fig. 3. M_e (■), reverse leakage current (▼) and photocurrent (●) measured on a 250- μm diameter InAs $p-i-n$ diode during the noise measurement at an intermediate $T = 200$ K.

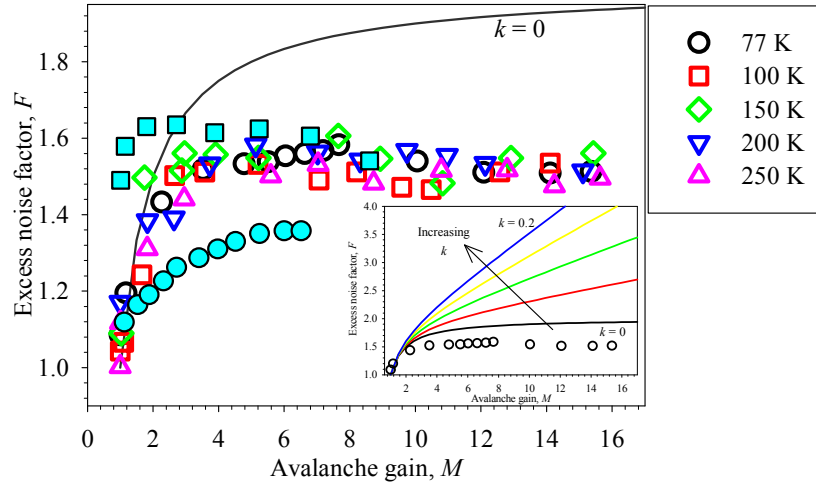


Fig. 4. F_e measured on the InAs p - i - n diode at 77, 100, 150, 200 and 250 K (opened symbols) under top illumination compared to previous results (closed symbols) at room temperature (square) [5] and 77 K (circle) [10]. Reference local model line of $k = 0$ (solid line). Inset shows the excess noise factors calculated using the local model for $k = 0$ to 0.2 with an increment of 0.05.

F_e of the InAs diode was measured at 77 to 250 K. They vary between 1.45 and 1.6 at $M_e > 3$ for this temperature range. The fluctuation in the measured data prevented us from establishing if there is any clear temperature dependence of F_e suggesting that within the accuracy of the measurements, F_e is only very weakly dependent on T . The results are summarized in Fig. 4.

3. Discussion

3.1 Avalanche gain characteristics

Figure 2 shows that from 77 to 295 K, M_e increases quite linearly with T at a given V_b . In wide bandgap semiconductors such as Si and GaAs, the reduced temperature lowers the number of phonon scattering events leading to a larger population of hot carriers that increases the impact ionization events. On the other hand in narrow bandgap materials, in which impact ionization can occur at energies close to E_g [26, 27], the role of minimum ionization energy is more significant at low electric fields. Consequently in InAs, with large Γ - X and Γ - L valley separation energies reported to be $\geq 2E_g$ [23, 26, 28], it is reasonable to assume that the temperature dependence of electron ionization threshold energy will dominate over that of phonon scattering. Therefore, assuming that the ionization threshold energy is proportional to E_g which increases with decreasing T , α may be expected to decrease with T , consistent with our measurement results.

The performance of a detector can be evaluated in term of its signal to noise ratio. In our InAs eAPDs the signal depends on the responsivity and M_e , while the noise is controlled dominantly by the multiplied dark current. To evaluate the performance of InAs eAPDs at different T , it is important to know the responsivity at the desired wavelength, the dark current and M . In our previous work we found that InAs eAPDs, without anti-reflection coating, exhibited temperature independent quantum efficiency of $\sim 50\%$ for radiation wavelengths from 1.3 to 2 μm at 77 and 295 K [29]. We have also reported that both bulk and surface leakage current components in InAs diode reduce rapidly with decreasing T [9]. Recently, reduced gain-normalized dark current density was reported for InAs p - i - n diode with graded p -doping. This is because the highly-doped p -region near the p -contact formed a larger energetic barrier to the minority electrons in the p -layer [8]. By decreasing the operating

temperature, it can be expected that much lower leakage current can be obtained from these graded InAs diodes, as reported in [9].

Table 1. Comparison between the Gain-Normalized Dark Current Densities and Avalanche Gains at a Bias Voltage of 12 V at 77, 200 and 295 K.

T (K)	295	200	77
Gain-normalized dark current density (A/cm^2) at 12 V	0.28	1.2×10^{-3}	1.7×10^{-5}
M_e at 12 V	18.2	11.8	7.0

It is clear that reducing temperature will reduce M_e . However the inset of Fig. 2 also shows that the rate of change of M_e with T , $\Delta M_e/\Delta T$ is dependent on the operating voltage. A larger $\Delta M_e/\Delta T$ was observed at a higher V_b . While establishing the trade-off between dark current and M_e reduction as a function of bias is not trivial, we observed that the dark current drops more rapidly than M_e as T decreases. For example as shown in Table 1, at $V_b = 12$ V the dark current reduces by > 2 and 4 orders of magnitude as T reduces from 295 to 200 and 77 K respectively. However M_e drops only by a factor of 1.5 and 2.6. Since the responsivity is temperature independent and the shot noise contributed by the dark current has to be lower than the amplifier's noise for the avalanche gain to be useful, cooling InAs eAPD is expected to improve its signal to noise ratio significantly.

3.2 Excess noise characteristics

F_e was found to show virtually no dependence on temperatures in Fig. 4 and M_e rises exponentially with no avalanche breakdown in Fig. 2, suggesting the absence of hole impact ionization and hence no band "resonance" effect was observed at the reported temperatures.

The previously reported F_e of InAs APDs at room temperature [5] and 77 K [10] are also plotted in Fig. 4 for comparison. The room temperature F_e was measured using a custom-built set-up [30] which could differentiate the photocurrent from the dark current and the result was very similar to those reported here from 77 to 250 K. However the 77 K result [10] is clearly lower than our current result. We believe that the lower F_e reported was due to a few experimental errors in the measurement set-up used previously. To increase the accuracy of the excess noise measurement, a few major improvements were done such as having APDs design suitable for high frequency measurement, the use of GSG probe and high frequency cables. These are crucial to ensure that the actual noise powers of the APDs are measured. Figure 5 shows an example of the measured F_e at $M_e = 10$, where the F_e are consistent throughout the measured frequencies from 10 to 300 MHz indicating there is no noise attenuation. Previous 77 K noise measurements were done using the d.c. probes of the low temperature probe station. The unshielded parts of the d.c probes could pick up external interfering signals. Inset of Fig. 5 shows the normalized frequency response of the probes which have power losses of ~ 3 and ~ 10 dB at 12 and 30 MHz respectively [31]. These were the frequencies at which the results were obtained for the previous 77 K measurements [10]. Hence these could be errors that lead to the underestimation of F_e .

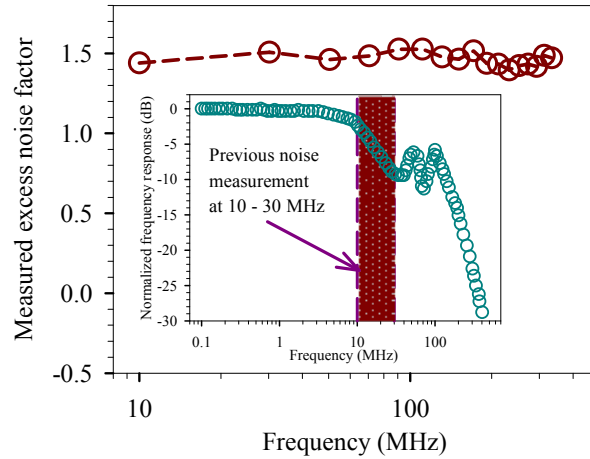


Fig. 5. An example of the measured F_e at $M_e = 10$ from 10 to 300 MHz. Inset shows the normalized frequency response of the DC-probe for the low temperature probe station [31].

The inset of Fig. 4 describes the variation of F with M in a local model [3] for $k = 0$ to 0.2, with $k = 0$ producing the lowest excess noise. From Fig. 4, the F_e of InAs eAPD is clearly lying below the lower limit of $k = 0$ in the local model. We attribute this very low F_e to the reduced randomness in the ionization path length due to the dead space effect. For APDs with $k = 1$, the mean ionization path length, $\langle l \rangle$ at high gain is comparable to W . Hence in this case d becomes comparable in length to $\langle l \rangle$ only when W is thin, usually significantly less than $1 \mu\text{m}$ [32]. However in the case of $k = 0$, $\langle l \rangle$ is much shorter than W so that multiple ionization events can occur to build up the avalanche gain within a single transit time. As a result the dead space effect is dominant even in APDs with $W \gg 1 \mu\text{m}$, such as in our InAs eAPD. Hence, αd , which is the ratio of d to $\langle l \rangle$ (since $1/\alpha = \langle l \rangle$), can be used as a measure of the dead space effect, with a higher value of αd indicating a more deterministic process [5, 33].

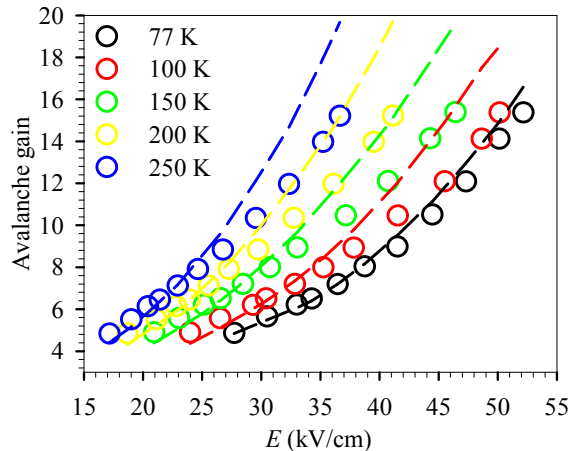


Fig. 6. Electric field dependent measured M_e (symbols) and the RPL simulated M_e (dashed-lines) from 77 to 250 K.

It is evident from the excess noise measurements that the effect of dead space is significant in InAs eAPDs with thick W . While the previously derived α using local model can predict M_e reasonably well [10, 34], this model is not appropriate for the prediction of F_e . Therefore, the nonlocal effect needs to be taken into account when modeling the InAs eAPDs regardless of its operating temperatures. We have attempted to fit the M_e and F_e results

reported here using the Random Path Length model [35]. F_e can be fitted reasonably well between 1.45 - 1.6 and the simulated trend of increasing M_e at a given bias with temperatures remain the same. However as shown in Fig. 6, the simulated M_e does not agree with the measured values especially at high electric fields. We believe this may be due to the gradual increase of electron impact ionization rate with energy. In InAs, E_g is substantially smaller than Γ -X and Γ -L valley separation energies such that most ionization events occur at the bottom of the conduction band. However due to the limited density of states in Γ valley of InAs the ionization rate increases gradually with energy and hence is described as soft ionization rate [26]. Therefore the single effective hard threshold used in this model, which assumes a dramatic or sharp increase in the ionization rate once the electron has travelled through the dead space, is not sufficient to model InAs APDs. An analytical band Monte Carlo similar to [26] is currently being developed to provide an accurate modeling of the results reported here for InAs eAPDs.

4. Conclusion

The impact ionization properties of InAs APD were investigated at $T = 77$ to 250 K by obtaining an accurate temperature dependence of M_e and F_e . The reducing M_e with reducing T at a fixed V_b suggests that the effects of the increase in ionization threshold energy, due to the increase in E_g , dominates over those due to the reduced phonon scattering.

Irrespective of the temperature, we demonstrated that the InAs eAPD could provide high gain with consistently low F_e , below that predicted by the local model. The discrepancy in the previous F_e results at 77 K was rectified by having APD design and experimental set-up suitable for high frequency measurements. For the reported electric field range, InAs APDs possess the eAPD characteristics with no observation of the impact ionization of holes. This suggests the absence of band “resonance” at the reported temperatures and electric field range of the InAs eAPD. From the excess noise results, we conclude that the effect of dead space is still significant in the impact ionization process of eAPDs with thick W . We found that the simple hard dead space model did not provide accurate modeling at high electric fields and hence, a more accurate model incorporating improved transport description is necessary.

Acknowledgments

The work reported in this paper was supported by the Engineering and Physical Sciences Research Council (EP/H031464/1). P. J. Ker would like to thank the Malaysian Public Service Department for the Ph.D studentship.